

Adaptive Multi-Band Multi-Mode Power Amplifier Using Integrated Varactor-Based Tunable Matching Networks

W. C. Edmund Neo, *Student Member, IEEE*, Yu Lin, Xiao-dong Liu, Leo C. N. de Vreede, *Senior Member, IEEE*, Lawrence E. Larson, *Fellow, IEEE*, Marco Spirito, *Student Member, IEEE*, Marco J. Pelk, Koen Buisman, *Student Member, IEEE*, Atef Akhnoukh, Anton de Graauw, and Lis K. Nanver, *Member, IEEE*

Abstract—This paper presents a multi-band multi-mode class-AB power amplifier, which utilizes continuously tunable input and output matching networks integrated in a low-loss silicon-on-glass technology. The tunable matching networks make use of very high Q varactor diodes ($Q > 100$ @ 2 GHz) in a low distortion anti-series configuration to achieve the desired source and load impedance tunability. A QUBIC4G (SiGe, $f_t = 50$ GHz) high voltage breakdown transistor ($V_{CBO} = 14$ V, $V_{CEO} > 3.6$ V) is used as active device. The realized adaptive amplifier provides 13 dB gain, 27–28 dBm output power at the 900, 1800, 1900 and 2100 MHz bands. For the communication bands above 1 GHz optimum load adaptation is facilitated resulting in efficiencies between 30%–55% over a 10 dB output power control range. The total chip area (including matching networks) of the amplifier is 8 mm².

Index Terms—Adaptive matching network, dynamic loadline, high efficiency, multi-band, multi-mode, power amplifier, RF adaptivity.

I. INTRODUCTION

IN ORDER TO fulfill the multi-band, multi-mode demands of today's cellular market, current handset implementations are based on parallel line-ups for the transmit and receive paths [Fig. 1(a)] with antenna duplexers and switches to meet the specific requirements of each communication standard. Next-generation wireless systems aim for size and cost reduction by utilizing only one or two adaptive transmit/receive paths to replace the parallel path concept [Fig. 1(b)]. Although conceptually simple, practical design considerations place severe design constraints and technology challenges on the adaptive circuit blocks required. For most of the circuit functions in the receive path, acceptable implementations have already been demonstrated [1]–[3]. Major challenges remain, however, in creating the tunable filters and adaptive power amplifiers (PAs) [4], [5]. To address these challenges we focus in this paper on

the implementation of an adaptive PA. Our aim is to improve the power-added efficiency (PAE) and provide adaptation of the operating frequency.

A. PA Requirements

The power amplifier stage in a mobile handset is considered to be one of the most power hungry components. As a result, the talk-time of a typical handset is restricted to several hours by the limited PA efficiency and battery performance. There are two basic constraints for a mobile system that are responsible for this limitation:

- the maximum output power required, related to transmitted power, when the handset is operated at a large distance from the base-station;
- the high linearity requirement of a modern wireless communication system, which translates to a power back-off condition of several dB for the output stage.

In traditional amplifier implementations, the linearity requirement typically results in the use of class-AB operation for the output stage [6], which provides a workable compromise between linearity and efficiency. When considering linearity, the class-AB output stage must be dimensioned in such a way that it can provide its peak output power without saturation. As a result, for a given peak output power (P_{peak}) and battery voltage (V_{cc}), the load impedance for a class-AB stage at the fundamental frequency is fixed to $R_L \approx 0.5 \cdot V_{cc}^2 / P_{peak}$.

Unfortunately, class-AB operation provides its highest efficiency only under maximum drive conditions. When operated at the required back-off level, due to linearity reasons for a given communication standard like (W)CDMA, a rather dramatic loss in efficiency occurs [7]. It is for these reasons that improving amplifier efficiency, while maintaining linearity, is currently a major research topic in wireless communications.

In linearity-focused research, the circuit is designed so that the resulting overall linearity performance of the PA module is improved. In this way, the active device can be operated closer to its peak-power capabilities and still be able to meet the linearity requirements. Pre-distortion is one technique that falls in this category. In pre-distortion (analog or digital) [8], the input signal is adjusted such that it compensates for the nonlinearities of the PA stage. Another increasingly utilized linearization technique is that of out-of-band termination [9]; here the impedances at baseband and second harmonic frequencies are

Manuscript received January 6, 2006; revised May 10, 2006. This work was supported in part by Philips Semiconductors, Philips Research, and the Dutch Technology Foundation (STW).

W. C. E. Neo, Y. Lin, X.-D. Liu, L. C. N. de Vreede, M. Spirito, M. J. Pelk, K. Buisman, A. Akhnoukh, and L. K. Nanver are with the DIMES Institute, Delft University of Technology, 2628 CT, Delft, The Netherlands.

L. E. Larson is with the University of California at San Diego, La Jolla, CA 92093 USA.

A. de Graauw is with Philips Semiconductors, 6534 AE Nijmegen, The Netherlands.

Digital Object Identifier 10.1109/JSSC.2006.880586

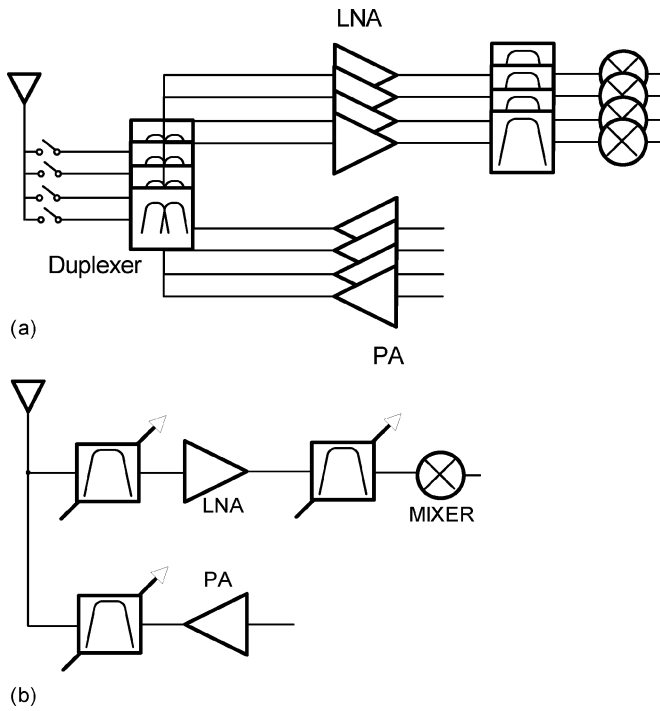


Fig. 1. (a) Traditional parallel path multi-band multi-mode approach based on static RF circuit blocks. (b) Simplified next-generation transceiver concept based on adaptive RF function blocks.

carefully tailored such that, through secondary mixing, the IM3 components resulting from third-order nonlinearities are cancelled. Although these techniques have proven to be effective, they do not improve the efficiency when the PA is operated at large power back-off levels.

Techniques that address the efficiency in the back-off mode are dynamic biasing [10] or regulation of the supply voltage of the output stage [11]. Dynamic biasing provides only modest improvements in efficiency, and supply voltage regulation requires an efficient DC-to-DC conversion, increasing system cost and complexity. An alternative for improved class-AB efficiency is load-line adjustment as a function of output power using an adaptive or reconfigurable output matching network. Typically, such a network is based on PIN-diode or PHEMT switching of matching elements like inductors, transmission-lines [5] or capacitors. In addition, MEMS capacitors are currently being considered for this application although they still have manufacturing and reliability issues and, when continuously tunable, linearity constraints [4], [12]–[16].

To overcome the limitations of existing adaptive matching solutions we aim to use varactor diodes for the continuous tuning of the characteristics of the matching network. Unfortunately, the classical problem related to varactor diodes is their distortion when a modulated signal is applied to their terminals, disqualifying them for linear applications. In [17] and [18], however, it was demonstrated that by stacking diodes in anti-series, one can obtain an almost “distortion-free” tunable capacitor. A logical idea would be to realize these structures in conventional silicon technology. However, the series parasitics related to such a varactor implementation (e.g., the resistance of the buried layer and

connecting metal fingers) would yield unworkable high losses for the intended capacitance values.

This parasitics-induced limitation can be overcome by realizing the “distortion-free” varactor concept on a glass substrate transfer technology (silicon-on-glass) [19], facilitating low-ohmic contacting of the intrinsic device at both front and back-side, providing ultra-low loss ($Q > 100$ @ 2 GHz) tunable capacitors which exhibit almost no distortion. This, combined with the use of thick metal layers (copper plated) for the realization of high Q inductors and transmission lines, facilitates the integration of high quality tunable integrated matching networks [20], which are adaptive in port impedance and operating frequency. Note that these integrated adaptive networks can play an important role for the realization of the next generation of adaptive transceivers [Fig. 1(b)]. To illustrate the feasibility of this approach, we have demonstrated in [24] an 1800 MHz QUBIC4G [23] bipolar PA with adaptive integrated input and output matching networks. Using these matching networks, high-efficiency performance has been obtained even at large power back-off conditions by adapting the load that the active device sees as a function of the output power. In this paper, we take the next step and combine the high-efficiency performance of the adaptive PA for full and back-off power levels with multi-band functionality.

This paper is organized as follows. In Section II, we review why we are able to achieve better power-efficiency performance at different power levels by changing the load impedance of the output stage. In Section III, we discuss the design, fabrication and characterization of the adaptive matching networks used in this work. In Section IV, we present the design of the complete PA module (active device and matching networks). The efficiency improvement for a single-tone signal as function of output power (impedance) is given at the different frequency bands to illustrate the improvement in power efficiency over a classical class-AB PA implementation. The conclusions are given in Section V.

II. STATIC LOAD-LINE MODULATION CONCEPT

When considering a normal class-B amplifier, the supply voltage (V_{cc}) and the load resistance (R_L) are fixed quantities in which R_L is set by the peak output. Since, for ideal class-B operation the max output voltage amplitude equals V_{cc} , when the device is delivering peak power, the output power can be written as

$$P_{out} = P_{col} = \frac{v_{col}^2}{2R_L} = \frac{V_{cc}^2}{2R_L}. \quad (1)$$

The maximum collector efficiency can be simply written for a sinusoidal signal as

$$\eta_{max} = \frac{P_{col}}{P_{dc}} = \frac{V_{cc} \cdot i_{col}}{2V_{cc} \cdot I_{dc}} = \frac{i_{col}}{2I_{dc}}. \quad (2)$$

Note that this expression only involves a ratio of currents and for sinusoidal signals this ratio equals $\pi/4$, which gives the theoretical efficiency of 78.5% for class-B amplifiers. Unfortunately,

at back-off power levels the voltage swing at the collector is only a fraction of the bias supply voltage V_{cc} . Inserting this back-off voltage level into the efficiency equation, we obtain

$$\eta = \frac{v_{\text{backoff}}}{2V_{cc}} \cdot \frac{i_{\text{col}}}{I_{dc}} = \frac{v_{\text{backoff}}}{V_{cc}} \cdot \frac{\pi}{4} = \sqrt{\frac{P_{\text{backoff}}}{P_{\text{peak}}}} \cdot 78.5\%. \quad (3)$$

We observe that the efficiency drops with the square root of the power back-off ratio. However, if R_L is changed such that the voltage swing at the collector is kept equal to the bias supply voltage, the power efficiency in (2) can be achieved at all power levels, and there is no drop in efficiency when the power is backed off. Although the considerations above apply to class-B operation, they can also be applied to class-E or class-F amplifiers, yielding a theoretical upper limit of 100% efficiency for all output power levels.

III. RECONFIGURABLE MATCHING NETWORK

In order to effectively change the loading impedance of the output stage as a function of the desired output power level, tunable matching networks are required. In this section, we discuss the basic requirements these networks must satisfy to obtain the desired PA functionality in terms of power control range and frequency tuning. Following that, we discuss the design of the matching network within the technology constraints and the resulting implementation with its measurement results.

A. Design Goal of Adaptive Matching Networks

For the implementation of our tunable matching network, we use uniformly doped varactors in a silicon-on-glass technology. To improve linearity, the anti-series configuration of two uniformly doped varactors [17], [18] is used. Note that this configuration is theoretically distortion-free when a high impedance is used for biasing the center node. Compared to other RF tunable components, these elements provide superior linearity, reliability, capacitance tuning speed and quality factor ($Q > 100$ @ 2 GHz), making them fundamental enabling components for wireless applications [18].

The currently available varactor devices in our silicon-on-glass process place the following design constraints on the reconfigurable matching network:

- effective capacitance tuning range of the varactor stack ($C_{\text{max}}/C_{\text{min}}$): < 2.5 ;
- control voltages: < 18 V (to avoid diode breakdown);
- no forward biasing of any of the diodes by the RF signal.

Although in principle, control voltages up to 18 V are required to obtain the full capacitance tuning range for this technology version, it is noted that the varactor diodes are always operated in reverse bias and therefore require practically no current. Consequently, the generation of these control voltages by DC-to-DC up-conversion is relatively straightforward without any severe requirement on conversion efficiency. The actual value of the control voltages depends on the intended capacitance control range and the RF voltage swing present in the matching network. By using a low Q matching network solution in combination with low impedance levels, one can improve the

power handling range of the design. With the above constraints in mind, we aim for the following specifications for the reconfigurable matching network:

- impedance transformation ratio > 10 ;
- continuously tunable with high tuning speed (20-MHz bandwidth);
- operating frequencies of 900, 1800, 1900, and 2100 MHz (covering the most important bands for handsets);
- losses < 1 dB for the whole input impedance tuning range;
- number of independent control voltages ≤ 2 ;
- high linearity (> 55 dBc at 1 W output power level);
- output power range from 0.1 to 1 W assuming a 3-V supply voltage;
- improved amplifier efficiency for power back-off conditions.

In order to meet these requirements, we need to determine the most promising network topology.

B. Choice of Adaptive Matching Network Topology

Since we aim for low-loss matching network implementations with only two control voltages, we limit the number of reactive elements in our analysis to a maximum of four. The networks considered in our analysis are given in Fig. 2. Variable inductors are composed of an inductor/varactor combination with a net positive reactance.

Of these networks, the L-type network is the simplest. In principle this configuration can provide impedance transformation up to the loading impedance of the network (50Ω). Unfortunately, to obtain an acceptable impedance transformation range, it requires a very large tuning range for its component values. A π -type matching network has one more element than a L-type network, which in principle allows a load termination to be transformed to any position within the Smith-chart. When using two L-type matching networks in cascade, we obtain the so-called two-stage ladder matching network. As with the π -type matching network, this topology allows an impedance transformation that covers the entire Smith chart. The advantage of the ladder network over the π -type network is that, for higher impedance transformation ratios, the Q of the two-stage network is significantly lower. Note that high Q conditions in the matching network give rise to increased losses and higher voltage swings, limiting the power handling capabilities.

When implementing a transformer or coupled line-based matching network, one suffers from the tradeoff between the impedance tuning range and coupling factor of the coils. As a result, high Q conditions are required to obtain the intended tuning range, yielding higher losses. All these matching networks yield large S_{21} phase variations (> 10 degrees over a 5 to 50Ω impedance range) when changing the impedance transformation by adjusting the network elements. When changed dynamically [21], [22], this phase variation appears as an AM-to-PM distortion and degrades the linearity of a dynamic load modulated amplifier when no compensating measures like digital predistortion are taken. If one wants to avoid the use of predistortion in this application, one can consider network

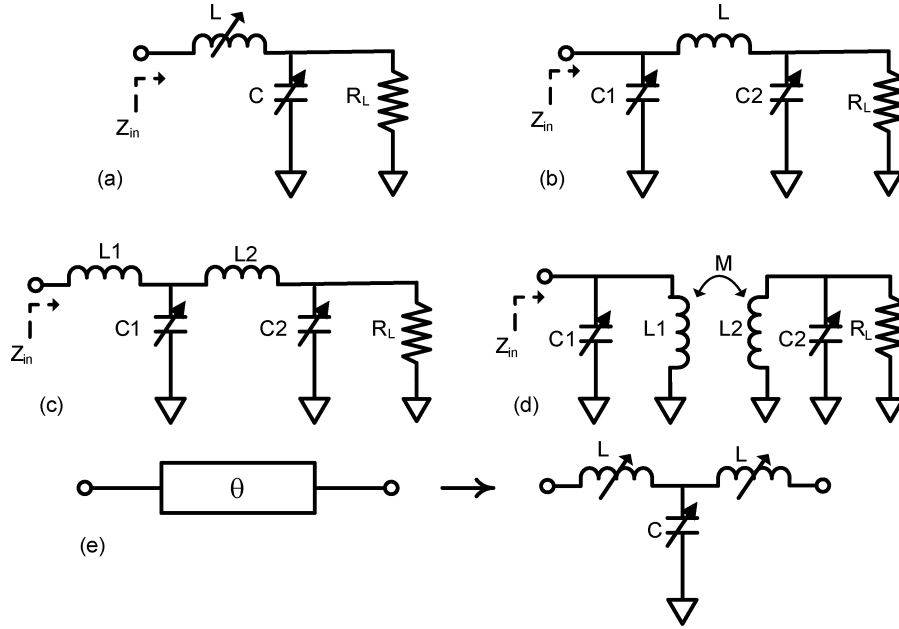


Fig. 2. Network topologies considered for the implementation of the adaptive matching network. (a) L-type network. (b) π -type network. (c) Two section L-type network. (d) Transformer coupled network. (e) Constant delay network.

TABLE I
EVALUATION OF MATCHING NETWORKS

Types of matching network	Impedance Ratio (>10)	Q at high transfer ratio	Complexity	Compactness
L	N	-----	Low	Good
Π	Y	Low	Low	Good
Two-stage ladder	Y	Lowest	Low	Good
Coupled line	Y	Very High	High	Moderate
Constant phase shift	Y	Low	Very High	Bad

solutions that provide no S_{21} phase variation when changing the impedance ratio. A $\lambda/4$ transmission transformer is such a network [Fig. 2(e)], which, for a limited bandwidth, can be approximated by its lumped equivalent. Consequently, by changing both the L and C simultaneously, one can vary the characteristic impedance while keeping the phase delay constant. This approach requires tunable inductors, which in principle can be implemented using a combination of an inductor and a capacitor. However, in practice this will result in increased losses making this topology less favorable compared to the other suggested matching network solutions.

The results of our analysis are summarized in Table I. Based on this table, the discussion above and the fact that we aim for static adaptive matching in this work, we have chosen the two-stage ladder network as the most suitable topology for our application. In the following section, we give the implementation details of this matching network and its measurement performance.

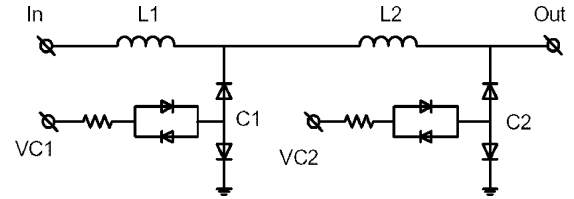


Fig. 3. Schematic diagram of the two-stage ladder network.

C. Implementation and Measurements of Adaptive Matching Networks

The schematic diagram of the two-stage ladder network is shown in Fig. 3. The tunable capacitors are composed of an anti-series configuration of two varactors, which form the so-called varactor stack (VS). A high value resistor and two diodes in anti-parallel configuration have been used to realize sufficiently high impedance for the varactor stack center tap to avoid linearity degradation for narrow tone spacing [18]. Each varactor stack is independently controlled for its effective capacitance through its center-tap voltage. The inductors can be realized either by coplanar waveguide [20] or bondwires; all reported matching networks are implemented using silicon-on-glass technology [19].

In our experiment, we used bondwires for the implementation of the inductors to facilitate tuning of the integrated matching network and simplify the connection to the active device. The values of the varactors and the inductance of the bondwires were chosen to achieve a large impedance control range at 1900 MHz and to obtain the lowest loss condition for the highest output power. The final bondwire dimensions were verified using a three-dimensional (3-D) field simulator. The layout and components values are given in Fig. 4 and Table II, respectively.

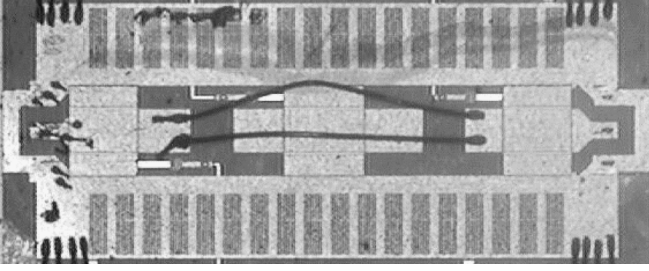


Fig. 4. Microphotograph of matching network using bondwires to realize the inductor.

TABLE II
ELEMENT VALUES OF OUTPUT MATCHING NETWORK

Element	Values
L_1	Length $\approx 600 \mu\text{m}$, radius wire $\approx 15 \mu\text{m}$, height $\approx 350 \mu\text{m}$, $L \approx 0.3 \text{ nH}$
Cj_{o1}	36 pF (zero bias)
L_2	Length $\approx 1870 \mu\text{m}$, radius wire $\approx 15 \mu\text{m}$, height $\approx 800 \mu\text{m}$, $L \approx 1.2 \text{ nH}$
Cj_{o2}	36 pF (zero bias)

The S-parameters of the matching network were measured using a HP8510C network analyzer. Fig. 5 shows the measured S_{11} of the integrated matching networks at 900, 1800, 1900, and 2100 MHz; this measurement illustrates the band-switching and impedance transformation capabilities of our adaptive matching network loaded with 50Ω at its output. The data of Fig. 5 is based on the on-wafer measured S-parameters of the device shown in Fig. 4. With this, we obtain the S_{11} data at the reference plane of the output of the active device. From Fig. 5 we observe that the S_{11} coverage in the Smith chart is very large for the higher frequency bands, providing a resistive impedance transformation range much larger than 10. Although the control range for the 900 MHz band is very limited, we can still approach the matching condition for the highest intended output power of the active device (28 dBm). Note that the 28 dBm optimum loading condition indicated on the Smith Chart assumes a lossless matching network. To compensate for the losses of the actual network, a slightly lower impedance has to be offered in practice.

One of the most important aspects of tuner design is to maximize the power gain ($P_{\text{out}}/P_{\text{in}}$) or minimize the losses of the structure. The definition of this gain is

$$G_p \text{ (dB)} = 10 \log_{10} \left(\frac{P_{\text{out}}}{P_{\text{in}}} \right) = 10 \log_{10} \left(\frac{|S_{21}|^2}{1 - |\Gamma_{\text{in}}|^2} \right). \quad (4)$$

Note that G_p is a more appropriate measure than G_{max} , since G_{max} assumes conjugate matching conditions at both input and output. (G_{max} was approximately -0.3 dB for all tuning values). Fig. 5 plots the measured loss contours up to -4 dB . The losses of these matching networks are caused by the limited Q of the inductors and the parasitic resistance of the varactor stacks.

The Q of the matching network was optimized to be low for the high power condition in order to avoid forward biasing

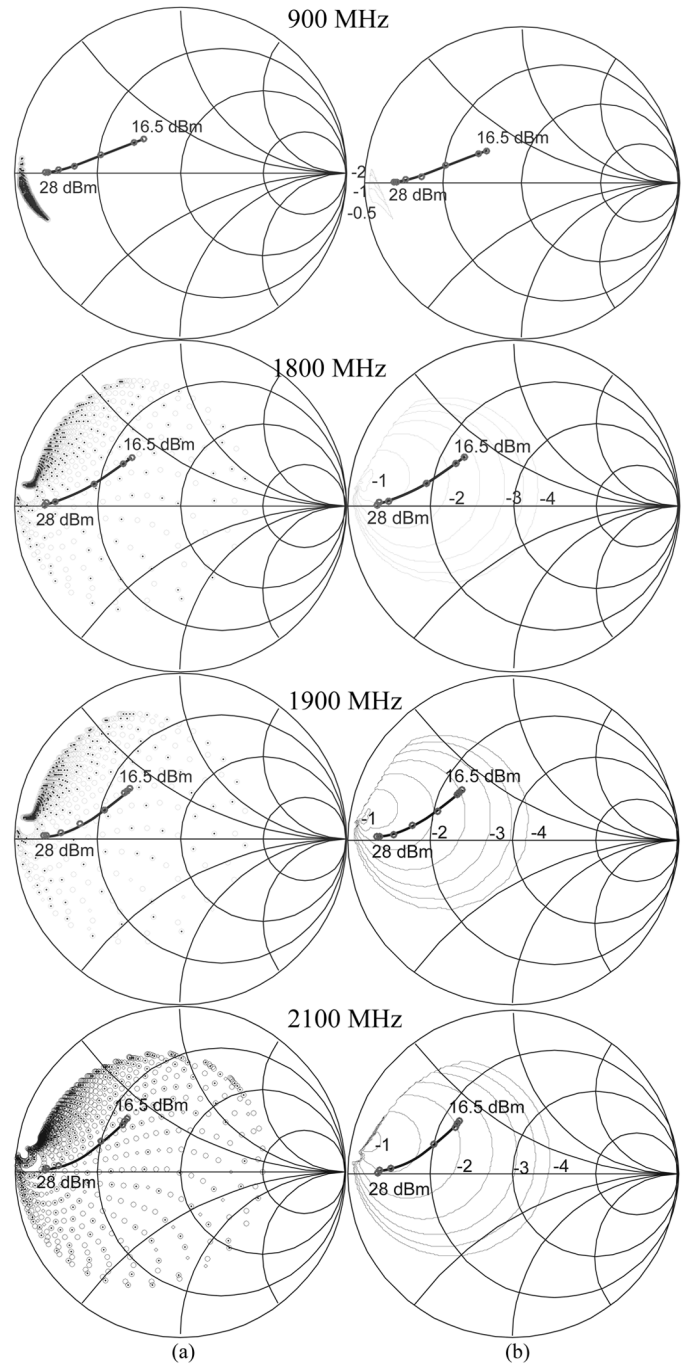


Fig. 5. (a) Measured S_{11} and (b) contours of constant G_p of the adaptive output matching network at 900, 1800, 1900 and 2100 MHz, the simulated optimum loading trajectories for the highest efficiency are indicated. $V_{\text{control}} < 18 \text{ V}$; required control voltage for the optimum load trajectory $< 10 \text{ V}$.

or voltage breakdown conditions of the varactors. As a consequence, the highest Q matching conditions are found for the low impedance ratio transformations, yielding higher losses.

In Fig. 5, the simulated optimum load trajectories as a function of output power, at the device reference plane, for maximum efficiency of the QUBIC device are also indicated. The expected gain and efficiency for the optimum load trajectory at 1800 MHz, assuming a lossless matching network is shown in Fig. 6. Note the significantly higher efficiencies achievable

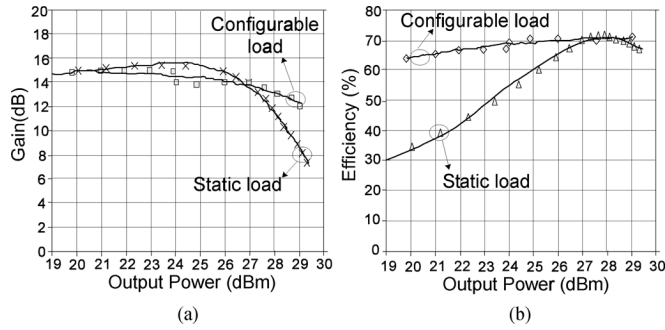


Fig. 6. Simulated (a) gain and (b) efficiency of the QUBIC device for the optimum loading trajectory of 1800 MHz.

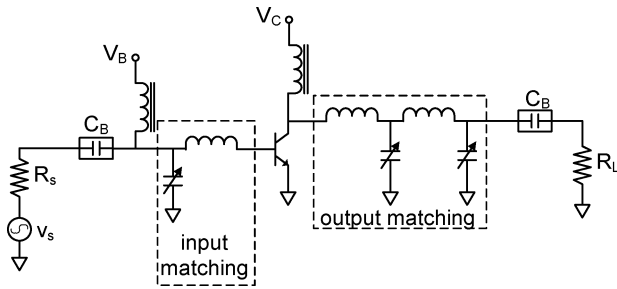


Fig. 7. Schematic of the adaptive power amplifier.

over a large power control range with the configurable load. The slight drop in efficiency at very high power back-off conditions can be partly explained by the remaining constant (RF power independent) part of the DC power consumption in class-AB operation. Also, the impact of device parasitics becomes more dominant in these large back-off conditions.

The large-signal performance of the varactor-based matching networks has been reported in [20] and the IM3 was better than 50 dBc ($f_c = 2$ GHz $\Delta f = 20$ MHz) with an output power control range of 17 to 27 dBm. Note that this performance meets the constraints of most communication standards for handsets. No forward biasing occurs for either of the diodes for RF powers up to 1 W. Simulations to investigate the effect of noise on the control voltages of the varactor show that a 10-mV sinusoid perturbation of 100 kHz on the control lines gives rise to spectral regrowth of -66 dBc relative to the carrier, which is sufficiently low for current communication standards.

These results demonstrate that the reconfigurable matching networks can provide the necessary impedance transformation when inserted into the PA module, with almost no degradation of the linearity due to modulation of the varactors or voltage fluctuation on the control lines.

IV. DESIGN OF A POWER AND FREQUENCY ADAPTIVE PA

Fig. 7 shows the schematic of our test circuit which consists of an active device (2-W SiGe HBT transistor with an f_t of 50 GHz [23]) between two tunable integrated input and output matching networks. We will utilize this configuration to verify the concept of static load-line modulation to improve the collector efficiency, as well as to achieve frequency-band switching.

At the input, a tunable L-type matching configuration, consisting of a shunt varactor and a series bondwire inductor, is used

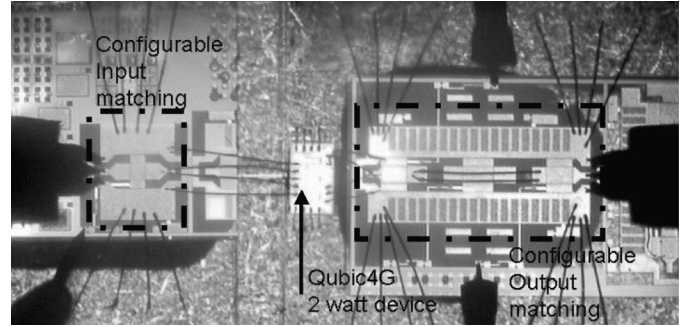


Fig. 8. Power amplifier with reconfigurable input and output matching network.

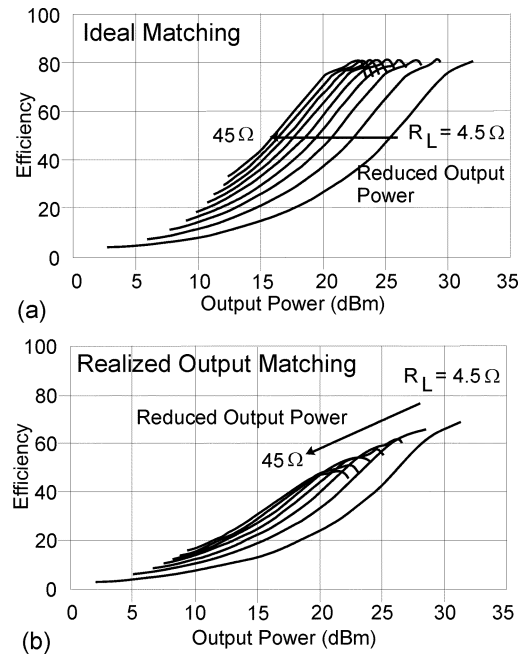


Fig. 9. Simulated power efficiency of an ideal class-B amplifier with (a) ideal matching network and (b) using the measured S-parameters of the fabricated matching network.

as pre-match for the active device. Fig. 8 shows a microphotograph of the final implemented PA module. The total chip area (active device + integrated matching networks) is 8 mm^2 .

From Section III, we saw that the output matching network exhibits variable losses as a function of impedance. To estimate the degradation in the power efficiency due to losses in the output matching network, we simulated an ideal class-B device along with the measured S-parameter values of the output matching network. Fig. 9(a) plots the simulated efficiency for different output loading conditions as a function of output power for a lossless matching network. In Fig. 9(b), this simulation has been repeated, but now using the *measured* losses of the adaptive output-matching network. As a consequence of the losses in the output matching network, the efficiency decrease is approximately 12% (from 80% to 68%) at high output power levels (30 dBm) and 30% (from 76% to 46%) at 10 dB back-off (20 dBm). Despite this, the efficiency is still much better at the 10 dB back-off point than the same amplifier implemented with a fixed output matching network.

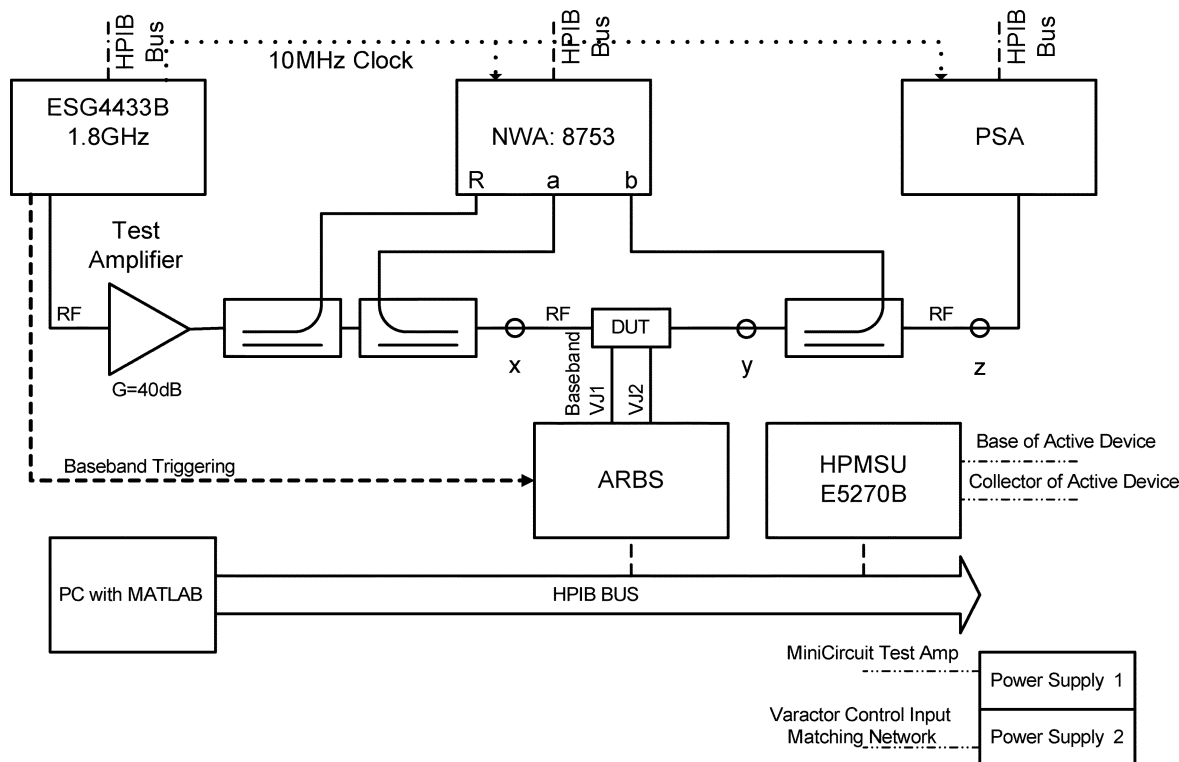


Fig. 10. Schematic of the test-bench for the adaptive PA.

A. Experimental Procedure

Although the optimum loading condition for the active device and input drive power level can be found through simulation, it is preferred to use an experimental approach to find the optimum control voltage for the varactors. Note that the best loading conditions are those that yield the highest efficiency for a given output power level. In the following experiments, we have used pulsed conditions for the biasing of the active device to avoid thermal problems. The schematic of the setup is given in Fig. 10.

Fig. 11 plots the measured gain versus output power for the 900, 1800, 1900, and 2100 MHz bands when the PA matching networks are fixed to the maximum output power settings at each frequency.

Fig. 12 plots the measured efficiency of the adaptive amplifier for the 900, 1800, 1900, and 2100 MHz bands. Two cases are described. First, the amplifier matching networks are fixed to their maximum output power settings at each frequency band (this result in the classical class-AB efficiency roll-off with back-off power). Second, for the 1800, 1900, and 2100 MHz bands, the efficiency is optimized for each P_{out} level, by providing the optimum combination of V_{C1} , V_{C2} , and P_{in} (Note that for the 900-MHz band, we do not have this freedom, since the impedance control range is very restricted [Fig. 5]).

The improvement in efficiency over the classical class-AB amplifier is clear and is typically more than 15%, resulting in an effective doubling of the efficiency when compared to the PA in power back-off using a fixed load, with minimal differences in the gain of the PA. As a result of this optimization, 30%–55% efficiency is achieved over a 10 dB range for the 1800, 1900,

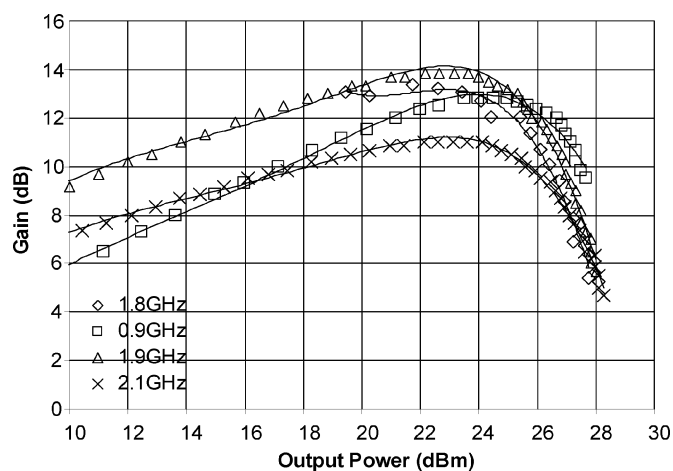


Fig. 11. Measured gain versus output power at 900, 1800, 1900, and 2100 MHz when the PA matching networks are fixed to their maximum output power settings for each band.

and 2100 MHz bands. Note that at 10 dB back-off, this efficiency exceeds the theoretical upper limit for class-B operation (24.8%). When considering the PAE, the gain should be taken into account, so in this case a drop in gain will affect its PAE, however, also for this parameter significant improvements are found in power back-off using the static loadline adjustments.

The varactor-based matching networks have been independently characterized for their linearity using a two-tone signal, yielding IM3 levels below -50 dBc for output powers up to 27 dBm output power ($f_c = 2$ GHz, $\Delta f = 20$ MHz) [20]. Consequently, the intermodulation products at the output of the adaptive PA is caused by the AM-AM and AM-PM distortion of

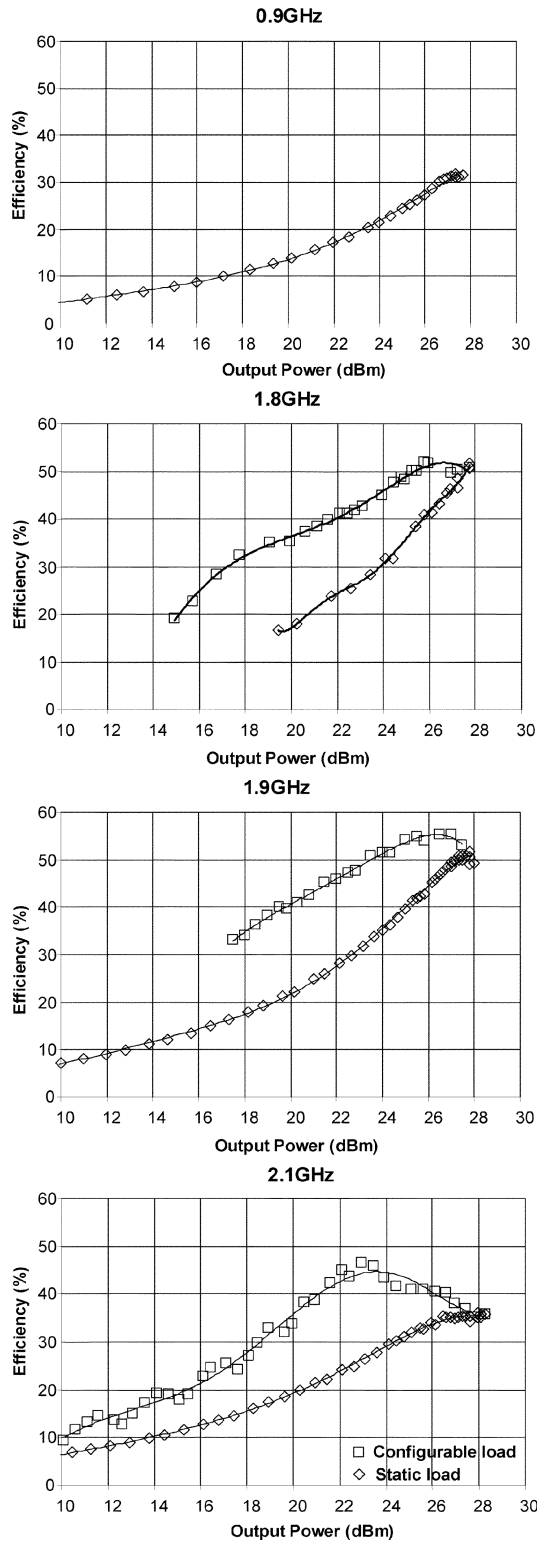


Fig. 12. Measured collector efficiency versus output power at 900, 1800, 1900, and 2100 MHz. First, the adaptive matching networks are fixed to the optimum maximum output power condition. Then, the output loading is optimized for efficiency at each power level.

the active device itself, in combination with secondary mixing products due to the nonoptimized second harmonic impedances at the input and output of the active device. Although the amplifier circuit itself was not optimized for linearity, two-tone testing

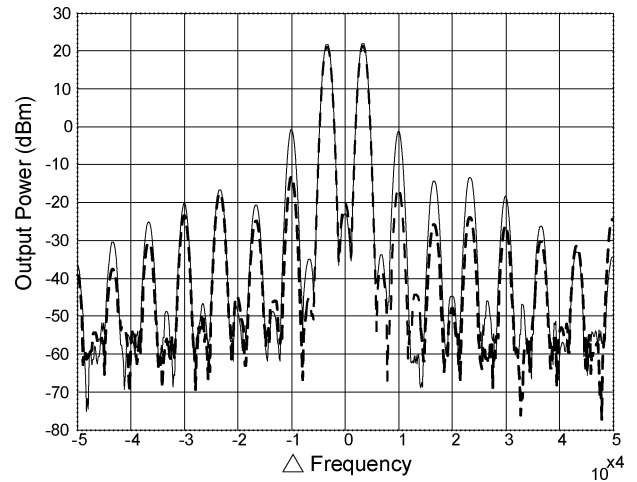


Fig. 13. Measured two tone linearity of the complete amplifier close to its maximum output power ($f_c = 900$ MHz, $\Delta f = 6.67$ kHz) solid line: without predistortion, broken line: with memoryless predistortion.

($f_c = 900$ MHz, $\Delta f = 6.67$ kHz) was performed on the complete amplifier close to its maximum power ratings (Fig. 13), which is a worst-case operating condition for linearity and is thus a good gauge of the overall linearity performance.

Note that the power of the fundamental tones is 22 dBm, yielding 25 dBm of average output power, which represents the maximum power level for unclipped two-tone operation [3 dB headroom, since $P_{\text{peak}} = 28$ dBm (Fig. 12)]. As expected, the linearity for this nonoptimized amplifier is not impressive ($\text{IM3} = -23$ dBc) owing to the poor AM-AM and AM-PM characteristics of the device itself. However, using digital predistortion (without including memory effect compensation), we improved the IM3 level to -35 dBc. By further reducing the memory effects in the experimental setup, this level can be further improved for larger tone spacing.

V. CONCLUSION

In this paper, for the first time, a multi-band multi-mode power amplifier, which is continuously tunable in operating frequency and output power level, is demonstrated. We have demonstrated 27–28 dBm output power at the 900, 1800, 1900, and 2100 MHz bands with very reasonable efficiencies. The integrated varactor-based matching networks are low-loss and provide low distortion due to the use of the anti-series varactor topology. The required control voltages in this amplifier for the intended load trajectory were restricted to 10 V. Since all varactors are reversed biased, the control of the adaptive network requires little DC power. The total chip area including integrated matching networks is restricted to 8 mm^2 , and can be made even more compact.

Although not addressed in this paper, varactor-based matching networks facilitate very fast tuning and are therefore capable to track the output stage loading conditions with the envelope of the modulated signal. This approach, known as dynamic load line modulation [21], [22], enables the PA to operate at its maximum efficiency at each point in time, yielding considerable efficiency improvements also for modulated signals with a high peak-to-average power ratio. This important

feature, combined with the demonstrated band-switching and static power control capabilities of this amplifier concept, motivates more research in this direction.

In view of this, it must be mentioned that although we have already achieved good results in terms of band switching, efficiency and power control range, there is still significant room for improvements: at the technology level, the design of the matching networks, and the mounting/grounding of the transistor and tunable matching networks. Consequently, even higher linearity and power levels can be obtained in future implementations. For these reasons, we consider this work as a starting point for the proposed techniques, opening up a new area for novel PA implementations.

ACKNOWLEDGMENT

The authors would like to thank R. Jos, F. van Straten, and P. Lok of Philips Semiconductors, Nijmegen, The Netherlands, for supporting this project. Special thanks go to all the people of the DIMES clean room facilities, TU Delft, The Netherlands, for developing the silicon-on-glass varactor technology and the assembly of the adaptive PA.

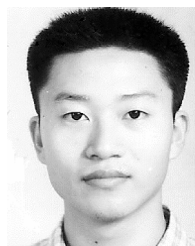
REFERENCES

- [1] J. Ryyanen, K. Kivekas, J. Jussila, A. Parssinen, and K. Halonen, "A dual-band RF front-end for WCDMA and GSM applications," in *Proc. IEEE Custom Integrated Circuits Conf.*, 2000, pp. 175–178.
- [2] D. Wang, X. Wang, A. Eshraghi, D. Chang, and P. Bacon, "A fully integrated GSM/DCS/PCS Rx VCO with fast switching auto-band selection," in *Proc. IEEE Radio and Wireless Conf.*, 2002, pp. 209–212.
- [3] A. Tasic, W. A. Serdijn, and J. R. Long, "Multi-standard/multi-band adaptive voltage-controlled oscillator," in *Proc. IEEE Radio Frequency Integrated Circuits Symp.*, 2004, pp. 135–138.
- [4] D. Qiao, R. Molino, S. M. Lardizabal, B. Pillans, P. M. Asbeck, and G. Jerinic, "An intelligently controlled RF power amplifier with a reconfigurable MEMS-varactor tuner," *IEEE Trans. Microw. Theory Tech.*, vol. 53, no. 3, pp. 1089–1095, Mar. 2005.
- [5] T. J. Hyeong, S. L. Hyun, S. C. Ik, and D. K. Chul, "Efficiency enhancement method for high-power amplifiers using a dynamic load adaptation technique," in *Proc. IEEE MTTT Int. Microwave Symp.*, 2005, pp. 2059–2062.
- [6] S. Cripps, *RF Power Amplifier for Wireless Communication*. Boston, MA: Artech House, 1999.
- [7] J. Deng, P. S. Gudem, L. E. Larson, and P. M. Asbeck, "A high average-efficiency SiGe HBT power amplifier for WCDMA handset applications," *IEEE Trans. Microw. Theory Tech.*, vol. 53, no. 2, pp. 529–537, Feb. 2005.
- [8] R. Marsalek, P. Jardin, and G. Baudoin, "From post-distortion to pre-distortion for power amplifiers linearization," *IEEE Commun. Lett.*, vol. 7, no. 7, pp. 308–310, Jul. 2003.
- [9] M. P. van der Heijden, M. Spirito, M. Pelk, L. C. N. de Vreede, and J. N. Burghartz, "On the optimum biasing and input out-of-band terminations of linear and power efficient class-AB bipolar RF amplifiers," in *Proc. IEEE Bipolar and BiCMOS Circuits and Technology Meeting*, 2004, pp. 44–47.
- [10] A. Khanifar, N. Maslennikov, R. Modina, and M. Gurvich, "Enhancement of power amplifier efficiency through dynamic bias switching," in *Proc. IEEE MTTT Int. Microwave Symp.*, 2004, pp. 2047–2050.
- [11] G. Grillo and D. Cristaudo, "Adaptive biasing for UMTS power amplifiers," in *Proc. IEEE Bipolar and BiCMOS Circuits and Technology Meeting*, 2004, pp. 188–191.
- [12] L. Yumin, D. Peroulis, S. Mohammadi, and L. P. B. Katehi, "A MEMS reconfigurable matching network for a class AB amplifier," *IEEE Microw. Wireless Compon. Lett.*, vol. 13, no. 10, pp. 437–439, Oct. 2003.
- [13] T. Vaha-Heikkilä, J. Varis, J. Tuovinen, and G. M. Rebiez, "A 20–50 GHz RF MEMS single-stub impedance tuner," *IEEE Microw. Wireless Compon. Lett.*, vol. 15, no. 4, pp. 205–207, Apr. 2005.
- [14] J. T. M. van Beek, M. H. W. M. van Delden, A. van Dijken, P. van Eerd, M. van Grootel, A. B. M. Jansman, A. L. A. M. Kemmeren, T. G. S. M. Rijks, P. G. Steeneken, J. den Toonder, M. Ulenaers, A. den Dekker, P. Lok, N. Pulsford, F. van Straten, L. van Teeffelen, J. de Coster, and R. Puers, "High-Q integrated RF passives and micromechanical capacitors on silicon," in *Proc. IEEE Bipolar and BiCMOS Circuits and Technology Meeting*, 2003, pp. 147–150.
- [15] J. Papapolymerou, K. L. Lange, C. L. Goldsmith, A. Malczewski, and J. Kleber, "Reconfigurable double-stub tuners using MEMS switches for intelligent RF front-ends," *IEEE Trans. Microw. Theory Tech.*, vol. 51, no. 1, pp. 271–278, Jan. 2003.
- [16] C. E. McIntosh, R. D. Pollard, and R. E. Miles, "Novel MMIC source-impedance tuners for on-wafer microwave noise-parameter measurements," *IEEE Microw. Guided Wave Lett.*, vol. 47, no. 2, pp. 125–131, Feb. 1999.
- [17] R. G. Meyer and M. L. Stephens, "Distortion in variable-capacitance diodes," *IEEE J. Solid-State Circuits*, vol. SC-10, no. 2, pp. 47–54, Feb. 1975.
- [18] K. Buisman, L. C. N. de Vreede, L. E. Larson, M. Spirito, A. Akhnoukh, T. L. M. Scholtes, and L. K. Nanver, "Distortion free varactor diode topologies for RF adaptivity," in *Proc. IEEE MTTT Int. Microwave Symp.*, 2005, pp. 157–160.
- [19] K. Buisman, L. K. Nanver, T. L. M. Scholtes, H. Schellevis, and L. C. N. de Vreede, "High-performance varactor diodes integrated in a silicon-on-glass technology," in *Proc. Eur. Solid-State Device Research Conf. (ESSDERC)*, 2005, pp. 117–120.
- [20] K. Buisman, L. C. N. de Vreede, L. E. Larson, M. Spirito, A. Akhnoukh, Y. Lin, X. Liu, and L. K. Nanver, "Low-distortion, low-loss varactor-based adaptive matching networks, implemented in a silicon-on-glass technology," in *Proc. IEEE Radio Frequency Integrated Circuits Symp.*, 2005, pp. 389–392.
- [21] F. H. Raab, "High-efficiency linear amplification by dynamic load modulation," in *Proc. IEEE MTTT Int. Microwave Symp.*, 2003, pp. 1717–1720.
- [22] G. Leuzzi and C. Micheli, "Variable-load constant efficiency power amplifier for mobile communications applications," in *Proc. Eur. Microwave Conf.*, 2003, pp. 375–377.
- [23] P. Deixler, R. Colclaser, D. Bower, N. Bell, W. de Boer, D. Szmyd, S. Bardy, W. Wilbanks, P. Barre, M. van Houdt, J. C. J. Paasschens, H. Veenstra, E. van der Heijden, J. J. T. M. Donkers, and J. W. Slotboom, "QUBiC4G: A $f_T/f_{max} = 70/100$ GHz 0.25 μ m low power SiGe-BiCMOS production technology with high quality passives for 12.5 Gb/s optical networking and emerging wireless applications up to 20 GHz," in *Proc. IEEE Bipolar and BiCMOS Circuits and Technology Meeting*, 2002, pp. 201–204.
- [24] W. C. E. Neo, X. Liu, Y. Lin, L. C. N. de Vreede, L. E. Larson, M. Spirito, A. Akhnoukh, A. de Grauw, and L. K. Nanver, "Improved hybrid SiGe HBT class-AB power amplifier efficiency using varactor-based tunable matching networks," in *Proc. IEEE Bipolar and BiCMOS Circuits and Technology Meeting*, 2005, pp. 108–111.



W. C. Edmund Neo (S'05) received the B.Eng. degree in electrical engineering from the National University of Singapore in 2002, and the M.Sc. degree in electrical engineering from the Delft University of Technology, The Netherlands, in 2004. In 2004, he joined the High Frequency Components and Technology group at the Delft University of Technology, where he is currently working towards the Ph.D degree in electrical engineering.

His research interest is in the area of novel circuit design techniques for high-efficiency and high-linearity RF power amplifiers.



Yu Lin received the BSc. degree in electrical engineering from Dalian Maritime University, China, in 2003, and the M.Sc. degree in microelectronics from Delft University of Technology, The Netherlands, in 2005.

Afterwards, he joined Broadcom Corporation, Bunnik, The Netherlands, and is currently involved in analog CMOS design. His interests are in analog and RF circuit design.



Xiaodong Liu received the B.S. degree from Jilin University, Changchun, China, in 2002, and the M.Sc. degree from Delft University of Technology, Delft, The Netherlands, in 2005, both in electrical engineering.

He is currently an Analog Design Engineer with Broadcom Netherlands involved in the design of mixed-signal circuits for communication applications. His areas of interest include RF and high-speed circuits.



Marco Spirito (S'01) received the M.Sc. degree *cum laude* in electrical engineering in 2000 from the University of Naples "Federico II", Naples, Italy.

In August 2000, he joined the Laboratory of High-Frequency Technology and Components in the Faculty of Electrical Engineering, Mathematics and Computer Science, Delft University of Technology, The Netherlands. He first worked there on the design and optimization of high-performance and rugged power amplifiers. Between 2002 and 2005, he focused on the development and implementation of advanced characterization setups for power amplifiers, such as passive, differential and active load-pull setups. In 2006, he joined the Department of Electronics and Telecommunications Engineering of the University of Naples "Federico II". His interests include characterization of highly linear PAs and development of advanced characterization tools and procedures for modern high-speed digital memory.

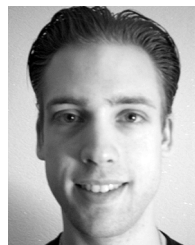
Mr. Spirito received the Best Student Paper Award for his contribution to the BCTM 2002 Conference.



Leo C.N. de Vreede (M'01–SM'04) was born in Delft, The Netherlands in 1965. He received the B.S. degree in electrical engineering from the Hague Polytechnic in 1988. He received the Ph.D. degree from Delft University of Technology in 1996.

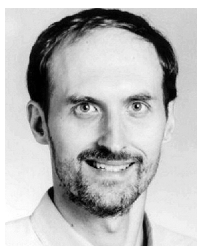
In 1988, he joined the Laboratory of Telecommunication and Remote Sensing Technology of the Department of Electrical Engineering, Delft University of Technology. From 1988 to 1990, he was involved in the characterization and physical modeling of CMC capacitors. From 1990 to 1996,

he worked on modeling and design aspects of HF silicon ICs for wideband communication systems. In 1996, he was appointed as Assistant Professor at the Delft University of Technology working on the nonlinear distortion behavior of bipolar transistors at the device physics, compact model, and circuit level, at Delft Institute of Microelectronics and Submicron Technology (DIMES). In the winter season of 1998–1999, he was a guest of the High Speed Device group at the University of San Diego, La Jolla, CA. In 1999, he became an Associate Professor, responsible for the Microwave Components Group of the Delft University of Technology. His current interest is technology optimization and circuit design for improved RF performance and linearity.



Marco J. Pelk received the B.S. degree in electrical engineering from the Hague Polytechnic in 2000.

In 2000, he joined the Laboratory of Electronic Components, Technology and Materials (ECTM) of the Department of Electrical Engineering, Delft University of Technology. From 2000 to 2002, he was involved in the implementation of compact and mixed-level device models for circuit simulation. Starting in 2002, he worked on the design of several components for a novel active harmonic load-pull system. He is also supporting other activities related to microwave measurements. His current interest is nonlinear device characterization and microwave circuit design.



Lawrence E. Larson (S'82–M'86–SM'90–F'00) received the B.S. and M. Eng. degrees in electrical engineering from Cornell University, Ithaca, NY, in 1979 and 1980, respectively, and the Ph.D. degree in electrical engineering and the MBA degree from the University of California at Los Angeles (UCLA), in 1986 and 1996, respectively.

From 1980 to 1996, he was with Hughes Research Laboratories, Malibu, CA, where he directed the development of high-frequency microelectronics in GaAs, InP, and Si/SiGe and MEMS technologies.

In 1996, he joined the faculty of the University of California at San Diego (UCSD), La Jolla, where he is the Inaugural Holder of the Communications Industry Chair. He is currently Director of the UCSD Center for Wireless Communications. During the 2000–2001 academic years, he was on leave with IBM Research, San Diego, CA, where he directed the development of RF integrated circuits (RFICs) for third-generation (3G) applications. During the 2004 to 2005 academic year he was a Visiting Professor at TU Delft in the Netherlands. He has authored or coauthored over 250 papers. He holds 31 U.S. patents.

Dr. Larson was the recipient of the 1995 Hughes Electronics Sector Patent Award for his work on RF MEMS technology. He was co-recipient of the 1996 Lawrence A. Hyland Patent Award of Hughes Electronics for his work on low-noise millimeter-wave high electron-mobility transistors (HEMTs), the 1999 IBM Microelectronics Excellence Award for his work in Si/SiGe HBT technology, and the 2003 IEEE Custom Integrated Circuits Conference Best Invited Paper Award.



Koen Buisman (S'05) received the M.Sc. degree in microelectronics from Delft University of Technology, The Netherlands, in 2004 and is currently pursuing the Ph.D. degree in the High Frequency Components and Technology group at the same university. For his Master's thesis, he worked on high-performance varactors for RF adaptivity. Currently, he is working on compact modeling of heterojunction bipolar transistors.



Atef Akhnoukh received the M.Sc. degree in electrical engineering from Aachen University of Technology (RWTH), Germany, in 1988.

From 1989 to 2003, he was with Philips Semiconductors, Nijmegen, The Netherlands, where he was involved in the design of amplifiers and transceivers. In 2003, he joined the microwave component group in the department of microelectronics and the Delft Institute of Microelectronics and Submicron technology (DIMES) within the Delft University of Technology.

His research interests include the characterization of RF/microwave devices and RF/analog circuit design.



Anton de Graauw received the M.S. degree in electrical engineering from the Technical University of Delft, The Netherlands, in 1993.

Currently, he is a Principal RF Engineer at the Innovation Center RF (ICRF) of Philips Semiconductors in Nijmegen, The Netherlands, where he is working on advanced RF modules for cellular systems.

In 1988, she joined the DIMES IC Process Research Sector as Bipolar Process Research Manager. She became Associate Professor and later Professor with the Faculty of Electrical Engineering, Mathematics and Computer Science, Delft University of Technology, detached at DIMES Technology Center in 1994 and 2001, respectively. Within the Laboratory of Electrical Components, Technology and Materials, she manages the research on advanced Si-based devices that is mainly directed towards optimization and development of high-frequency Si BJT/SiGe HBT devices and the integration of passives. This research involves technologies such as atmospheric-pressure/low-pressure (APCVD/LPCVD) epitaxy, dopant activation by excimer laser annealing, and substrate- transfer techniques.

Prof. Nanver has served on the committees of ESSDERC and BCTM.



Lis K. Nanver (S'80–M'83) received the M.Sc. degree in physics from the University of Aarhus, Aarhus, Denmark, in 1979. In 1982 she received the Dr. ing. degree from the Ecole Nationale Supérieure des Télécommunications, Paris, France, where she worked on the simulation of charge coupled device (CCD) structures. In 1987 she received the Ph.D. degree from the Delft University of Technology, Delft, The Netherlands, where she developed a medium-frequency bipolar field effect transistor (BIFET) process.